THE JOURNAL OF BIOLOGICAL CHEMISTRY VOL. 285, NO. 23, pp. 17993–18002, June 4, 2010
© 2010 by The American Society for Biochemistry and Molecular Biology, Inc. Printed in the U.S.A.

Identification and Characterization of Murine Mitochondria-associated Neutral Sphingomyelinase (MA-nSMase), the Mammalian Sphingomyelin Phosphodiesterase 5*[S]

Received for publication, January 12, 2010, and in revised form, April 5, 2010 Published, JBC Papers in Press, April 8, 2010, DOI 10.1074/jbc.M110.102988

Bill X. Wu, Vinodh Rajagopalan, Patrick L. Roddy, Christopher J. Clarke, and Yusuf A. Hannun[1]

From the Department of Biochemistry and Molecular Biology, Medical University of South Carolina, Charleston, South Carolina 29425

Sphingolipids play important roles in regulating cellular responses. Although mitochondria contain sphingolipids, direct regulation of their levels in mitochondria or mitochondria-associated membranes is mostly unclear. Neutral SMase (N-SMase) isoforms, which catalyze hydrolysis of sphingomyelin (SM) to ceramide and phosphocholine, have been found in the mitochondria of yeast and zebrafish, yet their existence in mammalian mitochondria remains unknown. Here, we have identified and cloned a cDNA based on nSMase homologous sequences. This cDNA encodes a novel protein of 483 amino acids that displays significant homology to nSMase2 and possesses the same catalytic core residues as members of the extended N-SMase family. A transiently expressed V5-tagged protein co-localized with both mitochondria and endoplasmic reticulum markers in MCF-7 and HEK293 cells; accordingly, the enzyme is referred to as mitochondria-associated nSMase (MA-nSMase). MA-nSMase was highly expressed in testis, pancreas, epididymis, and brain. MA-nSMase had an absolute requirement for cations such as Mg^{2+} and Mn^{2+} and activation by the anionic phospholipids, especially phosphatidylserine and the mitochondrial cardiolipin. Importantly, overexpression of MA-nSMase in HEK293 cells significantly increased *in vitro* N-SMase activity and also modulated the levels of SM and ceramide, indicating that the identified cDNA encodes a functional SMase. Thus, these studies identify and characterize, for the first time, a mammalian MA-nSMase. The characterization of MA-nSMase described here will contribute to our understanding of pathways regulated by sphingolipid metabolites, particularly with reference to the mitochondria and associated organelles.

Sphingolipids are appreciated as important structural components of cell membranes as well as critical regulators and mediators of many biological responses (1–3). Among the bioactive sphingolipids, ceramide has been extensively studied and identified as an important bioactive molecule in regulation of cell growth arrest, differentiation, apoptosis, and inflammation (4, 5). The levels and turnover of sphingolipids are regulated by several enzymes that play essential roles in regulation of their signaling effects. Sphingomyelinase (SMase)[2] or sphingomyelin phosphodiesterase (SMPD; EC 3.1.4.12) produces ceramide from the hydrolysis of sphingomyelin (SM), and considerable evidence has implicated SMase in regulating stress-induced ceramide production (5–7). The SMases have been classified into three different groups according to their catalytic pH optima: acid SMase, alkaline SMase, and neutral SMases (N-SMases), respectively.

To date, three N-SMases have been identified and cloned in mammals: nSMase1 (SMPD2), nSMase2 (SMPD3), and nSMase3 (SMPD4). Among the three enzymes, nSMase1 and nSMase2 were identified according to remote sequence similarity with bacterial SMase (8). Although nSMase1 exhibits *in vitro* SMase activity, it showed no effects on SM or ceramide levels when overexpressed in MCF-7 cells but rather had effects on lyso-PAF levels (9). Nonetheless, a recent study has suggested that nSMase1 can function as an *in vivo* SMase in some instances (10). In contrast, nSMase2 possesses both *in vitro* and *in vivo* activity, increasing ceramide levels when overexpressed (11, 12). The enzymatic activity of nSMase2 is Mg^{2+}-dependent and is activated by anionic phospholipids such as phosphatidylserine (PS). Moreover, nSMase2 has been implicated in a number of processes including the cellular response to cytokines and oxidative stress, growth arrest, development, and cell death (12–15). Unlike nSMase1 and nSMase2, nSMase3 was identified using the peptide sequence of a partially purified bovine protein (16). Although found to have very low sequence homology to the other N-SMase proteins, nSMase3 is also Mg^{2+}-dependent and is also activated by PS.

Recent insight into the functional roles of nSMases has come from the development of knock-out (KO) mice. The nSMase2 KO mice are characterized by a form of dwarfism most visibly manifested in the skeleton with the long bones found to have

* This work was supported, in whole or in part, by National Institutes of Health Grant GM 43825 (to Y. A. H.).

The nucleotide sequence(s) reported in this paper has been submitted to the GenBank™/EBI Data Bank with accession number(s) GU144514.

[S] The on-line version of this article (available at http://www.jbc.org) contains supplemental Fig. 1 and Table 1.

[1] To whom correspondence should be addressed: Dept. of Biochemistry and Molecular Biology, Medical University of South Carolina, 173 Ashley Ave., Charleston, SC 29425. Tel.: 843-792-9318; Fax: 843-792-4322; E-mail: hannun@musc.edu.

[2] The abbreviations used are: SMase, sphingomyelinase; N-SMase, neutral sphingomyelinase; MA-nSMase, mitochondria-associated nSMase; SMPD, sphingomyelin phosphodiesterase; SM, sphingomyelin; EST, expressed sequence tag; PS, phosphatidylserine; PA, phosphatidic acid; PC, phosphatidylcholine; PG, phosphatidylglycerol; PE, phosphatidylethanolamine; PI, phosphatidylinositol; CL, cardiolipin; KO, knock-out; ER, endoplasmic reticulum; RT-PCR, reverse transcription-PCR; PBS, phosphate-buffered saline; MES, 4-morpholineethanesulfonic; PAF, platelet-activating factor.

short stature and deformation (17). This report took on greater significance when the *fro/fro* mouse, a model of osteogenesis imperfecta, was found to carry a mutation in the *SMPD3* gene resulting in an inactive enzyme (18), thus suggesting a role for nSMase2 in regulation of bone homeostasis. However, despite these findings, no clear abnormality was observed in other tissues. Moreover, neither nSMase1 nor nSMase2 KO mice nor nSMase1-nSMase2 double KO mice appear to possess abnormalities in SM levels (17). Consequently, it is important to clarify the role of each SMase in cells and various tissues. Furthermore, it is essential to identify any undiscovered N-SMase, which may be important for SM metabolism and ceramide function.

Mitochondria contain a variety of sphingolipids, including ceramide and SM (19–21). Ceramide has also been implicated in mitochondria-mediated apoptosis (22–24). However, the direct regulation of sphingolipids in mitochondria or mitochondria-associated membranes is mostly unclear with few reports detecting changes in mitochondrial ceramide in response to induction of apoptosis (25, 26). This lack of information on SMase and other sphingolipid-regulating enzymes in mitochondria has significantly handicapped efforts to delineate signaling pathways in this organelle that involve sphingolipids. Notably, in yeast, the mammalian N-SMase orthologue Isc1p has been localized to both mitochondria and ER and is important for yeast cell growth (27). In contrast, nSMase2 localizes to the plasma membrane and Golgi, whereas nSMase3 localizes to the Golgi and ER (16, 28). More recently, a zebrafish N-SMase was identified in zebrafish that localized at least partly to mitochondria on overexpression (21). Taken together, this suggests the potential existence of a mitochondria-associated N-SMase in mammals, which could be a key enzyme for sphingolipid metabolism.

In this study, we have cloned and characterized a novel murine SMase (SMPD5) that shares significant sequence similarity with nSMase2 and zebrafish mitochondrial SMase and has comparable biochemical properties, indicating that it is a member of the extended N-SMase family. Uniquely among mammalian nSMases, the SMase localizes to both mitochondria and ER. Thus, we propose to name the enzyme as mitochondria-associated neutral SMase (MA-nSMase). Importantly, overexpression of MA-nSMase resulted in significantly increased ceramide with a concomitant decrease of SM level, demonstrating its role in the regulation of cellular sphingolipids. Thus, these studies identify and characterize, for the first time, a mammalian MA-nSMase, with implications for the metabolism of sphingolipids associated with the mitochondria.

EXPERIMENTAL PROCEDURES

Materials—[Choline-*methyl*-^{14}C]SM was provided by the Lipidomics Core Facility at the Medical University of South Carolina. All other lipids were purchased from Avanti Polar Lipids. Goat anti-rabbit and goat anti-mouse antibodies were acquired from Santa Cruz Biotechnology. All other reagents were purchased from Sigma unless otherwise stated.

MA-nSMase Sequence Identification, Analysis, and cDNA Cloning—A tBLASTn search using the zebrafish mitochondrial nSMase and nSMase2 amino acid sequences identified several partial mouse cDNA sequences from the Expressed Sequence Tags (dbEST) database, including, BB615725.1, CF983093.1, BU583488.1, BY705974.1, CF197814.1, and BX516030.1. A further BLAST search using the identified EST sequences scanning the genomic sequence data bank revealed a sequence (NC000081) in mouse chromosome 15. To clarify the 5′ mouse MA-nSMase sequence, two oligonucleotides were synthesized based on the EST sequences (for primer sequence information, see supplemental Table 1). As several EST sequences were from the testis cDNA library, a mouse testis Marathon-ready cDNA (Clontech) was purchased for identification of the MA-nSMase sequence. Rapid amplification of cDNA ends was used to amplify the 5′ ends from the mouse cDNA according to the manufacturer's instructions. Further, a 1.5-kb cDNA containing the full-length coding region was amplified using the same testis cDNA and *Pfu* polymerase (Stratagene). PCR mixtures were first incubated at 94 °C for 3 min and then amplified for 45 cycles at 94 °C for 45 s, at 64 °C for 1 min, and at 72 °C for 3 min. The PCR product was sequenced and verified in independent PCR reactions. To express the MA-nSMase, the full-length coding sequence without stop codon was further amplified and then cloned into pcDNA3V5/His-topo vector (Invitrogen) following the manufacturer's instructions.

Real Time RT-PCR—Total RNAs from various mouse tissues were isolated using the Qiagen mini kit for total RNA extraction. cDNA was synthesized from 1 μg of total RNA using SuperScript II reverse transcriptase (Invitrogen). Real time RT-PCR was performed on an iCycler system (Bio-Rad) using SYBR Green PCR reagents (Bio-Rad). The first step of RT-PCR was performed at 95 °C for 3 min. Cycles ($n = 40$) consisted of a 15-s melt at 95 °C followed by 60 s at 55 °C. The final step was a 60-s incubation at 55 °C. Reactions were performed in triplicate. The β-actin gene was used as an internal reference control to normalize relative levels of gene expression. Real time PCR results were analyzed using Q-Gene® software (29), which expresses data as mean normalized expression. Mean normalized expression is directly proportional to the amount of RNA of the MA-nSMase relative to the amount of RNA of the β-actin.

Cell Culture and cDNA Transfection—HEK293 (ATCC CRL-1573) and MCF-7 (ATCC HTB-22) cells were cultured in Eagle's minimum essential medium or RPMI 1640 (Invitrogen), respectively. Cells were transfected using Lipofectamine 2000 (Invitrogen) according to the manufacturer's protocol at 37 °C in a humidified 5% CO_2 incubator. HEK293 cells were cultured in minimum Eagle's medium supplemented with 10% fetal bovine serum. DNA transfection was performed using Lipofectamine 2000 reagent (Invitrogen) according to the manufacturer's instructions.

Western Blot Analysis—The cells were collected in lysis buffer (25 mM Tris; pH 7.4, 1 mM EDTA, 1× protease inhibitor mixture (Roche Applied Science)) and homogenized by brief sonication. The homogenate was taken for protein determination using the BCA assay (Bio-Rad Laboratories). Twenty μg of total proteins from each lysate were loaded onto a 4–20% gradient SDS-polyacrylamide gel, subjected to electrophoresis, and then transferred to polyvinylidene difluoride membranes. The blots were probed using 1:2000 dilution of primary antibody followed by horseradish peroxidase labeled secondary

antibody (1:5000 dilution) (Santa Cruz Biotechnology). The signals were detected using ECL chemiluminescence reagents (Pierce). The antibodies against V5 were from Invitrogen. The β-actin antibody was purchased from Sigma.

Assays of Neutral Sphingomyelinase Activities—In vitro N-SMase enzymatic assays were performed as described previously with modifications (12). Briefly, cells were collected and lysed as described above, and 25 μg of proteins were used for each activity reaction. The final volume was adjusted to 200 μl. Each reaction mixture contained 50 mM Tris (pH 7.5), 5 mM $MgCl_2$, 0.1% Triton X-100, 2.5 mM dithiothreitol, 100 μM (6.5 mol %) PS, and 100 μM [choline-*methyl*-^{14}C]SM. For the pH optimum determination, the substrate was dissolved in 100 mM of the following buffers: acetate buffer (pH 4.0–5.5), MES buffer (pH 5.7–6.3), Tris buffer (pH 7.0–8.5), and glycine-NaOH buffer (pH 9.0–10.0). To determine the cation effects, neutral SMase activity was measured at various concentrations of $MgCl_2$, $MnCl_2$, $CaCl_2$, $ZnCl_2$, $FeCl_2$, or $CuCl_2$. For kinetics determination, 12.5 μM (0.8 mol %) to 400 μM (25.8 mol %) SM was used as a substrate for the activity assays. The kinetic parameters, V_{max} and K_m, were calculated using GraphPad Prism software. To determine the phospholipid effects on activity, 6.5 mol % of PS or other phospholipids (including phosphatidic acid (PA), phosphatidylcholine (PC), phosphatidyl-ethanolamine (PE), phosphatidylglycerol (PG), phosphatidylinositol (PI), and cardiolipin (CL)) was included in the reaction. After incubation for 0.5 h at 37 °C, the reaction was stopped by adding 1.5 ml of chloroform/methanol (2:1) followed by adding 400 μl of water. Phases were separated by centrifugation at 2000 × *g* for 5 min. By subjecting 500 μl of the upper phase to scintillation counting, SMase activity was determined by quantification of the amount of released radioactive phosphocholine.

PC-Phospholipase C and Lyso-PAF-Phospholipase C Assays—Assays were performed as described previously (9) with some modifications. The assay mixture was the same as N-SMase assay described above except that the reaction mixture contained 100 μM [choline-*methyl*-^{14}C]PC or [1-*O*-octadecyl-^{3}H]lyso-PAF instead of SM. After 30 min of incubation at 37 °C, the lipid was extracted by the method of Bligh and Dyer and separated by TLC in solvent system (chloroform/methanol/2 N NH_4OH 60:35:5). The TLC plates were sprayed with autoradiography enhancer (PerkinElmer Life Sciences) and exposed to film at −80 °C for 5 days. The bands corresponding to monoacylglycerol and diacylglycerol were scraped from the TLC plate for liquid scintillation counting.

Immunostaining and Confocal Microscopy—HEK293 or MCF-7 cells were grown on 35-mm glass-bottom culture dishes (MatTek). Transient transfection of plasmids (1 μg/dish) was performed using Effectene reagent (Qiagen) according to the manufacturer's recommendations. At 24 h after transfection, cells were washed with PBS and fixed with 3.7% formaldehyde for 10 min. Following fixation, cells were permeabilized for 5 min with 100% methanol at −20 °C and then blocked in 2% human serum (Jackson ImmunoResearch Laboratories) in PBS for 30 min at room temperature. Anti-Hsp60, anti-Tom20 (Santa Cruz Biotechnology), anti-giantin (Covance), or anti-calreticulin antibodies were co-incubated with anti-V5 antibody (Invitrogen). Incubations were performed in 2% human serum at 1:100 dilutions for 2 h at room temperature. Following primary antibody treatment, cells were washed three times with PBS, probed with fluorescent secondary antibody (1:200 anti-rabbit 555, 1:200 anti-mouse 488, 60 min, room temperature), and washed three times with PBS. Cells were stored at 4 °C under PBS prior to being viewed on a Zeiss LSM 510 Meta confocal microscope.

Liquid Chromatography/Mass Spectrometry Analysis of Endogenous SM and Ceramides—After 18 and 36 h of transfection with control pcDNA3 or MA-nSMase-pcDNA3 vector, the cells were harvested for SM and ceramide measurement. Sphingolipid analysis was performed in the Lipidomics Core Facility of the Medical University of South Carolina, using electrospray ionization/tandem mass spectrometry on a Thermo Finnigan TSQ 7000 triple stage quadrupole mass spectrometer, operating in a multiple reaction monitoring positive ionization mode (30). Each sample was normalized to its respective total protein levels.

Statistical Analysis—Results are expressed as the mean ± S.D. Comparisons among groups were made by Student's *t* tests. A *p* value of 0.05 or less was considered as statistically significant.

RESULTS

Cloning and Sequence Analysis of Mouse MA-nSMase Sequence—The cloned full-length mouse MA-nSMase cDNA consists of 1449 bp at the coding region (GenBank™ accession number GU144514). This open reading frame encodes a predicted protein of 483 amino acid residues (Fig. 1*A*) with a calculated molecular mass of 53,868 Da and an isoelectric point of 8.58. The MA-nSMase protein also retained significant motifs and amino acids essential to cation binding and catalytic activity, including the P-loop like domain and the key catalytic residues Asp-470 and His-471 (Fig. 1*A*) (27). Hydrophobicity and transmembrane domain analysis found a short sequence in the N-terminal region (amino acids 77–99) that is highly hydrophobic and is predicted to form a transmembrane helix (Fig. 1, *A* and *B*). The global GenBank search showed that mouse MA-nSMase is not identical to any identified gene but has high sequence homology with a number of EST clones. This cDNA also matches with the genome sequence from mouse chromosomes, revealing its chromosome location at 15D3. Moreover, phylogenetic analysis revealed (Fig. 1*C*) that the deduced mouse MA-nSMase protein has homology with other nSMases with the highest sequence homology shown to nSMase2 (50.6% similarity) and the zebrafish mitochondrial SMase (54.2% similarity) (Fig. 1*C*). Interestingly, the zebrafish SMase shares higher homology (58.5% similarity) to nSMase2 than to MA-nSMase. In summary, the sequence information revealed that the identified cDNA and the enzyme clearly belong to the extended family of N-SMases.

Tissue-specific Expression of the MA-nSMase mRNA—Next, the tissue-specific expression of mouse MA-nSMase mRNA was examined by real time RT-PCR (Fig. 2). As can be seen, expression levels varied among tissues with the highest expression found in testis, pancreas, epididymis, and brain. Significant levels of mRNA were also detected in spleen, thymus, and skin,

whereas the lowest mRNA levels were detected in stomach, intestine, colon, liver, lung, kidney, heart, ovary, and bladder. Additionally, a database search found MA-nSMase cDNA (EST) sequences in lymphatic tissue, thymus node, mammary gland, stem cells, and embryos at various stages. The expression pattern of MA-nSMase suggests that this enzyme may play important roles in reproductive, neuronal, developmental, and immune functions.

The MA-nSMase cDNA Encodes a Protein with in Vitro N-SMase Activity—Having identified a cDNA that encodes a putative mammalian SMase, it next became important to confirm that the encoded protein is indeed a functional SMase. Accordingly, a V5-tagged cDNA was transfected into HEK293 and MCF-7 cells. By Western blot, no signal was detected in empty vector pcDNA3-transfected cells, whereas a band with a molecular mass of about 50 kDa was detected in the cDNA-overexpressing cells (Fig. 3*A*). The band detected closely matched the calculated molecular mass of the predicted protein. To establish that the cloned protein functions as an nSMase, activity assays on vector-transfected and cDNA-transfected cells were performed. As can be seen, there was significantly greater N-SMase activity in the SMase-transfected cells than the control cells (Fig. 3, *B* and *C*). This confirms that the encoded protein possesses *in vitro* SMase activity. To determine whether the protein possessed enzymatic activity against lyso-PAF (as with nSMase1) or other lipids as substrates (such as PC), activity assays were performed. However, no significant activity was observed against these other substrates (data not shown). Taken together, these results demonstrate that the cDNA encodes an ~50-kDa protein that possesses *in vitro* N-SMase activity.

Subcellular Localization of the MA-nSMase Protein—Given the high similarity of MA-nSMase with both nSMase2 and the zebrafish

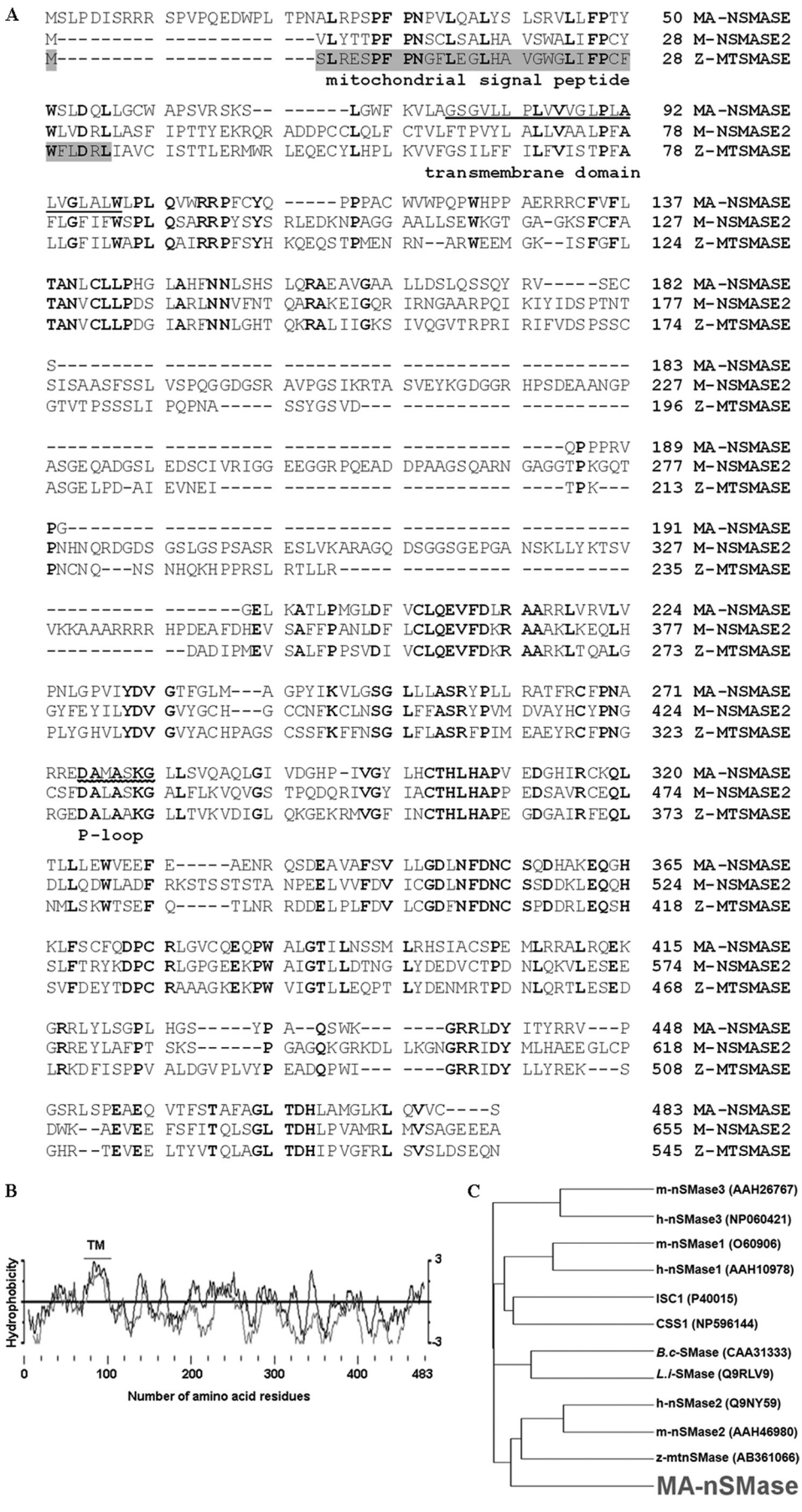

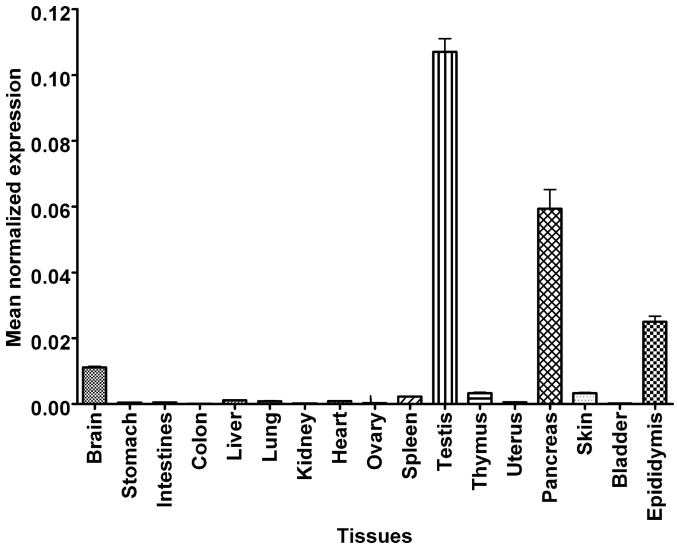

FIGURE 2. **Distribution of MA-nSMase mRNA in mouse tissues.** Total RNAs from various mouse tissues were isolated, and cDNA was synthesized from 1 μg of total RNA. Real time RT-PCR was performed using primers specific to MA-nSMase. β-Actin was used as an internal reference control to normalize relative levels of gene expression. Real time PCR results were expressed as mean normalized expression. The values are expressed as the mean ± S.D. ($n = 3$).

mitochondrial SMase, it became important to determine the subcellular localization of the new nSMase. Accordingly, the V5-tagged protein was transiently expressed in both MCF-7 (Fig. 4*A*, supplemental Fig. 1*A*) and HEK293 (Fig. 4*B*, supplemental Fig. 1*B*) cells. Cells were co-stained with V5 and antibodies against various subcellular markers. In both cell lines, confocal microscopy revealed that this protein was partly co-localized with the mitochondrial marker HSP60, suggesting that this protein localized to mitochondria. This was further confirmed with Tom20, a mitochondrial outer membrane marker. Interestingly, MA-nSMase showed a doughnut pattern of mitochondria that overlapped much more closely with TOM20 than with HSP60, suggesting that MA-nSMase is a mitochondrial membrane protein and not a matrix protein. Moreover, the protein also showed some overlapping signals with the ER marker calreticulin. However, overlay with the Golgi marker giantin demonstrated no significant co-localization. Taken together, these results demonstrate that MA-nSMase is localized to both mitochondria and ER.

Biochemical Characterization of MA-nSMase—Having confirmed that the cloned cDNA encodes a functional *in vitro* SMase, we next wanted to characterize the biochemical properties of the enzyme. For this, the activity of MA-nSMase was measured using lysates from HEK293 cells transiently transfected with MA-nSMase cDNA or an empty vector as control. As shown in Fig. 5*A*, the optimal activity of MA-nSMase was found in the neutral range with maximum activity at pH 7.5, confirming that this enzyme should be classified as an N-SMase. In contrast, there was comparable activity of vector control and SMase-overexpressing cells at the acid range of pH 4.0–6.0, suggesting that the new SMase has no acid SMase activity. Additionally, as the SMase activity of the vector control cells was very low at the neutral and alkaline pH range, this provided a low background for further analysis of the enzymatic properties of MA-nSMase in the overexpressing HEK293 cells. We next examined the kinetics of MA-nSMase activity (Fig. 5*B*) and found that the enzyme followed classical Michaelis-Menten kinetics displaying an apparent K_m of 14.3 ± 1.3 mol % and a V_{max} of 370.3 ± 16.8 nmol/h/mg of protein.

The metal ion dependence of the N-SMase activity was also analyzed. Accordingly, several cations including calcium, manganese, iron, copper, and zinc were substituted for magnesium in the *in vitro* assay. As can be seen, the N-SMase activity of MA-nSMase-overexpressing cells was strongly dependent on Mg^{2+} and Mn^{2+} with Mn^{2+} showing a higher stimulation (Fig. 5*C*). In contrast, calcium, copper, iron, or zinc did not support MA-nSMase activity. These results are very comparable with other members of the extended N-SMase family.

Anionic phospholipids were previously shown to function as activators of other mammalian N-SMases. Accordingly, the effect of phospholipids on MA-nSMase activity was also examined. At 100 μM (6.5 mol %), PG, PS, and CL strongly induced activity by ~8-, 15-, and 23-fold, respectively (Fig. 6*A*). In contrast, other phospholipids such as PA, PC, PE, and PI had minimal effects on MA-nSMase activity. Further analysis demonstrated that CL and PS can activate MA-nSMase in a dose-dependent manner with CL showing a lower K_a and a higher V_{max} (Fig. 6*B*). Overall, these results indicate that MA-nSMase has comparable biochemical properties with other N-SMase family members.

Modulation of SPL Levels by Overexpression of MA-nSMase in HEK293 Cells—Thus far, it has been shown that the MA-nSMase cDNA encodes a protein with *in vitro* N-SMase activity. Therefore, it became very important to confirm that MA-nSMase also possessed *in vivo* N-SMase activity and could modulate levels of SM and ceramide when overexpressed in cells. Accordingly, HEK293 cells were transiently transfected with MA-nSMase or empty vector, and both SM and ceramide levels at 18 and 36 h after transfection were assessed by mass spectrometry (Fig. 7). Results showed that MA-nSMase expression significantly increased total ceramide levels by 34% at 18 h and 93% at 36 h after transfection (Fig. 7*A*). At 18 h after transfection, many ceramide species were significantly increased with several unsaturated ceramides (C18:1, C20:1, C22:1)

FIGURE 1. **Sequence analysis of mouse MA-nSMase.** *A*, alignment of the deduced amino acid sequences of mouse MA-nSMase, mouse nSMase2, and zebrafish mitochondrial SMase (*Z-MTSMASE*). The sequences were aligned by the GCG Pileup program. Identical residues in all the three sequences are indicated by *bold characters*. The mitochondrial signal peptide in zebrafish mitochondrial SMase is *highlighted*. The predicted transmembrane domain and p-loop like domain are *underlined*. *B*, hydrophobicity profile of mouse MA-nSMase. The deduced amino acid sequence of MA-nSMase was analyzed by the method of Kyte-Doolittle (*dark line*) and by the Goldman method (*light line*) for hydrophobicity plotting. The predicted transmembrane (*TM*) domain is indicated. *C*, evolutionary relationships between MA-nSMase and other nSMases. A phylogenetic tree of various nSMases was plotted by the GCG program using the Kimura protein distance correction. The length of each *horizontal line* in the tree is proportional to the difference of the amino acid sequences. The nSMase sequences are from human (*h*), mouse (*m*), *Bacillus cereus (B.c)* and *Listeria ivanovii (L.i)*. The ISC1 and CSS1 sequences are from *Saccharomyces cerevisiae* and *Schizosaccharomyces pombe*.

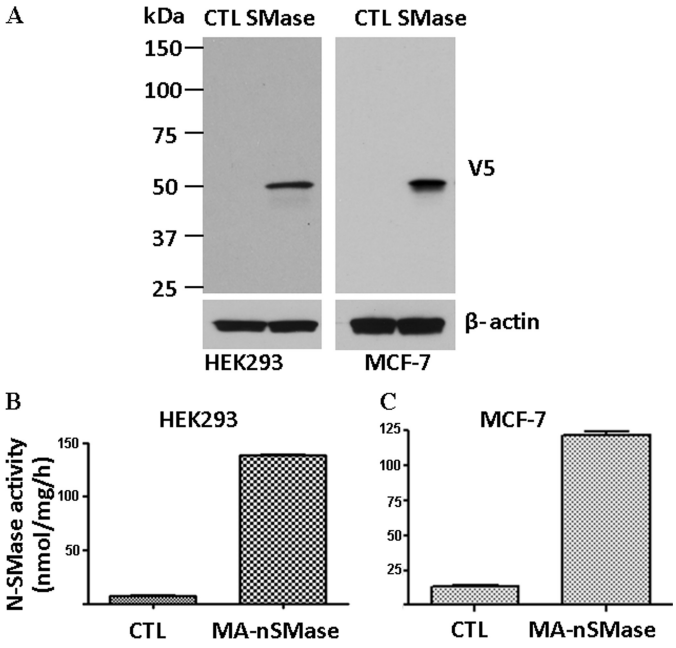

FIGURE 3. **Overexpression of the MA-nSMase in mammalian cell lines.** HEK293 and MCF-7 cells were transfected with an expression construct of mouse MA-nSMase. *A*, the expression of MA-nSMase was detected by Western blot analysis with a polyclonal antibody against V5. *CTL*, control. The N-SMase activity of the overexpressed enzyme was detected in both HEK293 (*B*) and MCF-7 cells (*C*). The values are expressed as the mean ± S.D. ($n = 3$).

showing the largest changes (Fig. 7, *B* and D). However, no significant changes were observed in dihydro-C16 ceramide or some of the very long chain ceramides, C24, C26, and C26:1-ceramides, suggesting that the corresponding SM might not be the favorable substrates for MA-nSMase in cells. At 36 h, all ceramides measured showed significant increases, with the largest -fold change (4-fold) observed for C20:1 ceramide (Fig. 7, *C* and *D*). Consistent with the ceramide data, MA-nSMase induced a significant decrease of total SM levels at 18 h after transfection (Fig. 8*A*), and this was observed for the majority of SM species (Fig. 8*B*). However, unlike with ceramides, only modest changes in SM levels were observed at 36 h after transfection, and with some SM species, levels were even partially recovered (Fig. 8, *C* and *D*). This is very likely due to cellular compensation. Nevertheless, these results demonstrate that MA-nSMase can modulate both SM and ceramide levels when overexpressed in cells and thus confirm that MA-nSMase is a functional N-SMase *in vitro* and *in vivo*.

DISCUSSION

In the present study, we have identified a cDNA encoding a novel murine nSMase. As the enzyme localizes in and around the mitochondria, we propose to refer to this enzyme as mitochondria-associated nSMase. Molecular characterization and biochemical analysis revealed that MA-nSMase is a member of the larger N-SMase family sharing biochemical properties with other family members but displaying distinct subcellular localization and tissue distribution. The characterization of the molecular properties of MA-nSMase described here will facilitate studies of its regulation and contribute to our understanding of signaling pathways mediated by sphingolipid metabolites, particularly with reference to the mitochondria and associated organelles.

MA-nSMase was identified and cloned from mouse tissue according to sequence similarity with nSMase2 and zebrafish SMase. Although there was no significant sequence homology to nSMase3, MA-nSMase displayed significant homology to nSMase2 (Fig. 1), and it possesses the same catalytic core residues (6) as nSMase1, nSMase2, ISC1, and other members of the extended N-SMase family. Overexpression of MA-nSMase in

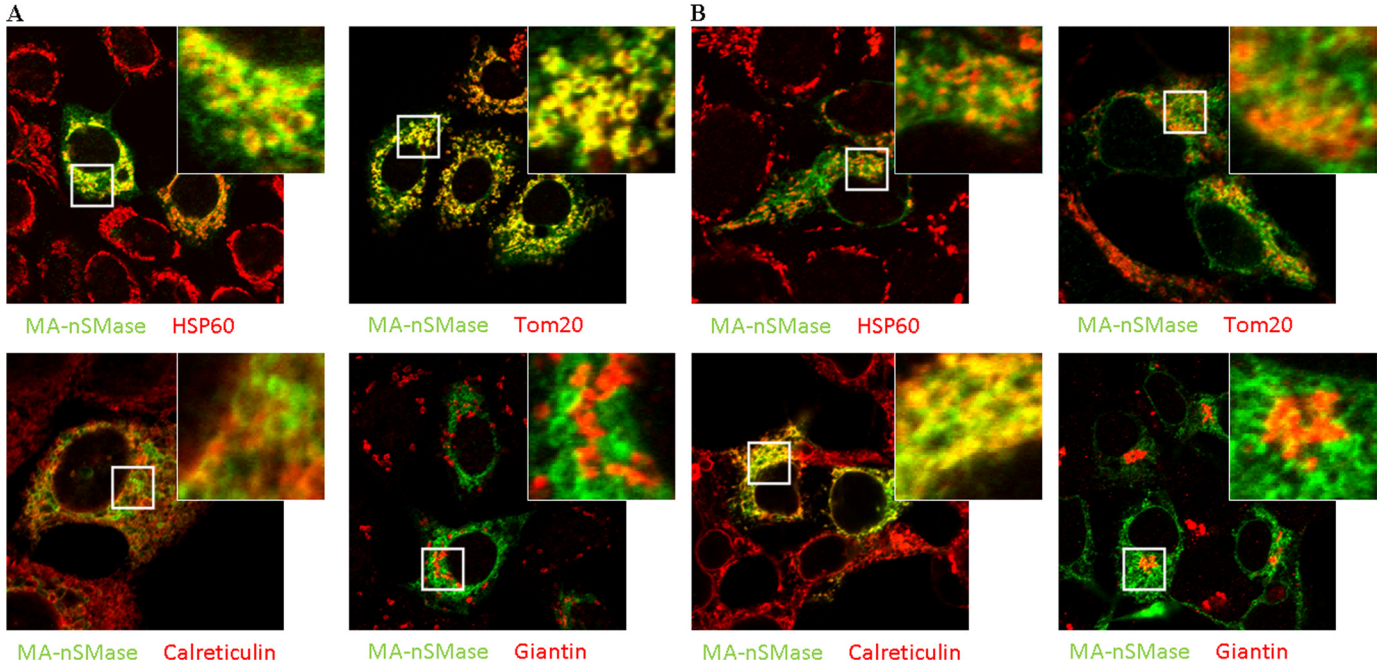

FIGURE 4. **Subcellular localization of mouse MA-nSMase.** *A* and *B*, MCF-7 (*A*) and HEK293 (*B*) cells were transfected with MA-nSMase expression vector. After 24 h, the cells were fixed and co-stained with an antibody against V5 (*green*) for MA-nSMase signal and antibodies against various subcellular markers (*red*), including HSP60 and Tom20 (mitochondrial markers), calreticulin (ER marker), and giantin (Golgi marker) and then subjected to confocal microscopic observation. The co-localization signals were observed as *yellow* or *orange*.

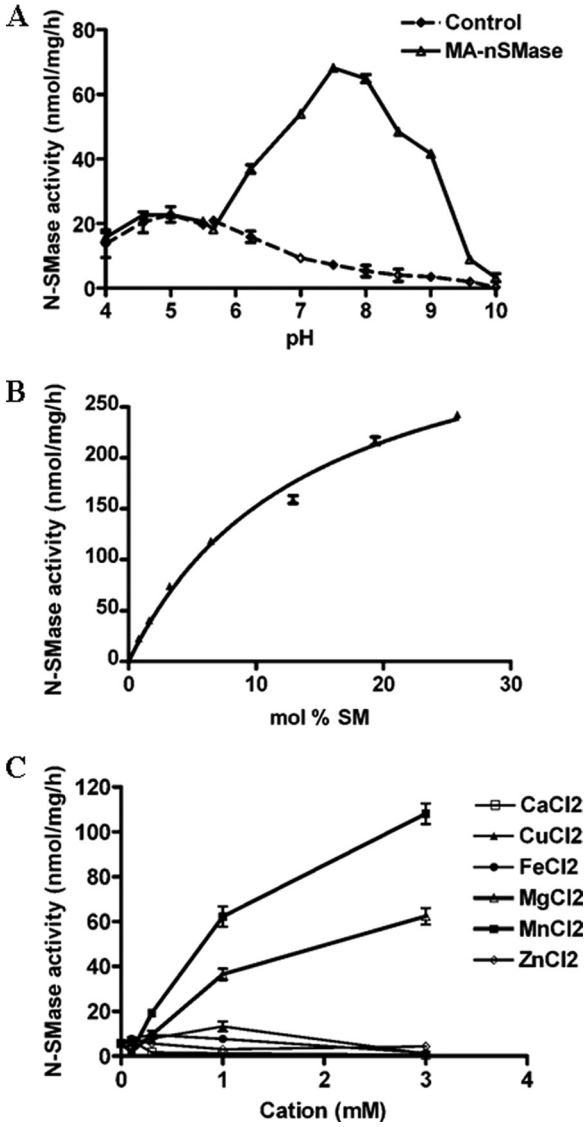

FIGURE 5. **Characterization of MA-nSMase expressed in HEK293 cells.** *A*, pH dependence of MA-nSMase activity. The SMase activity MA-nSMase was measured using 25 μg of protein from cells transfected with the MA-nSMase expression construct or with empty vector. The pH was adjusted by the addition of the indicated buffers at a final concentration of 100 mM. The following buffers were used: acetate buffer (pH 4.0–5.5), MES buffer (pH 5.7–6.3), Tris buffer (pH 7.0–8.5), and glycine-NaOH buffer (pH 9.0–10.0). *B*, N-SMase activity toward increasing concentrations of SM substrate. *C*, cation effects were assayed using 6.5 mol % (100 μM) of SM and 6.5 mol % of PS. N-SMase activity was measured at various concentrations of $MgCl_2$, $MnCl_2$, $CaCl_2$, $ZnCl_2$, $FeCl_2$, or $CuCl_2$. *B*, the results are averages of triplicates. *A* and *C*, the data are the averages of duplicates. The values are expressed as the mean ± S.D. The data are representative of at least two independent experiments.

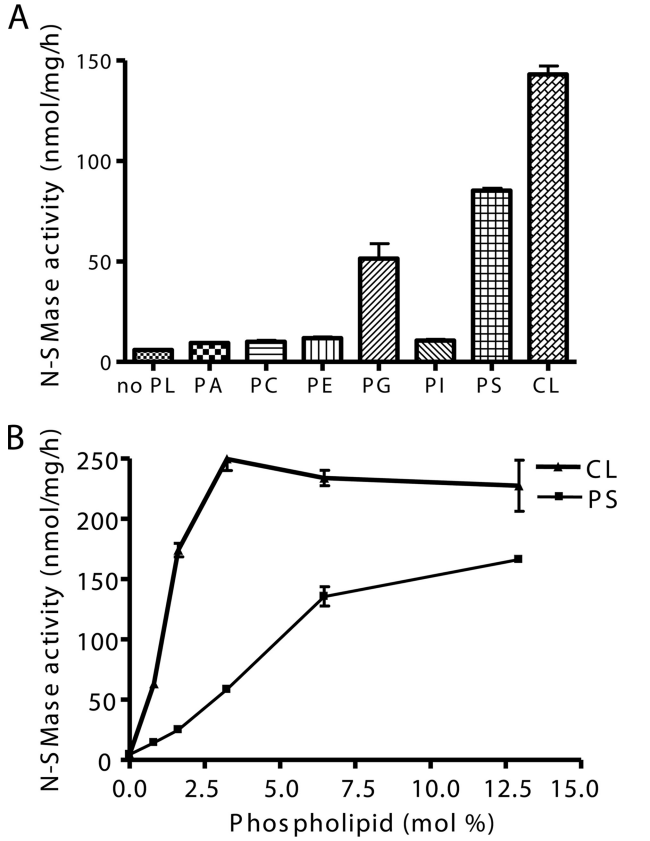

FIGURE 6. **Effects of phospholipids on N-SMase activity.** The N-SMase activity was measured using 6.5 mol % of SM. *A*, the indicated dioleoyl-phospholipids were delivered at a final concentration of 6.5 mol % (100 μM), and enzyme activity was assayed in the presence of PS or other phospholipids (PA, PC, PE, PG, PI, or CL). *B*, the activity of MA-nSMase on SM was measured at various concentrations of PS or CL. The data are the averages of duplicates from at least two independent experiments. The values are expressed as the mean ± S.D.

HEK293 cells significantly increased *in vitro* N-SMase activity, indicating that the identified cDNA encodes a functional SMase (Figs. 3 and 5). Importantly, no significant activity of MA-nSMase was observed against other potential substrates, such as lyso-PAF and PC. Finally, MA-nSMase had similar biochemical properties as other nSMases including an absolute requirement for cations, specifically Mg^{2+} and Mn^{2+} for full activity, and was activated by the anionic phospholipids PS and CL. Therefore, based on sequence comparison and biochemical properties, we conclude that MA-nSMase clearly belongs to the extended N-SMase family.

Subcellular localization results indicated that MA-nSMase strongly localized to the mitochondria of MCF-7 cells and partially localized to the mitochondria of HEK293 cells (Fig. 4). Additionally, MA-nSMase also partially localized to the ER. Notably, there was more overlap of MA-nSMase with the ER marker in HEK293 cells than in MCF-7 cells. Thus, the subcellular distribution of MA-nSMase (between mitochondria and ER) may be cell type-specific. This localization is notably different from all other mammalian N-SMases but, remarkably, is similar to what was previously reported for the yeast nSMase homologue ISC1, also a member of the extended N-SMase family. Interestingly, in *S. cerevisiae*, ISC1 localizes predominantly to the ER during exponential growth but appears to relocalize to the mitochondria following the diauxic shift, when metabolism switches from glycolytic to aerobic (31, 32). With this in mind, it would be of great interest to determine whether the localization of MA-nSMase is also subject to such regulation. It is also important to determine whether the localization of MA-nSMase dictates its roles within the cell. These studies are currently underway in our laboratory. As proteins are synthesized in the ER, the possibility that overexpression may result in accumulation of MA-nSMase in ER cannot be completely excluded.

This study also suggests a potential role for the mitochondria in activation of MA-nSMase by anionic phospholipids (Fig. 6).

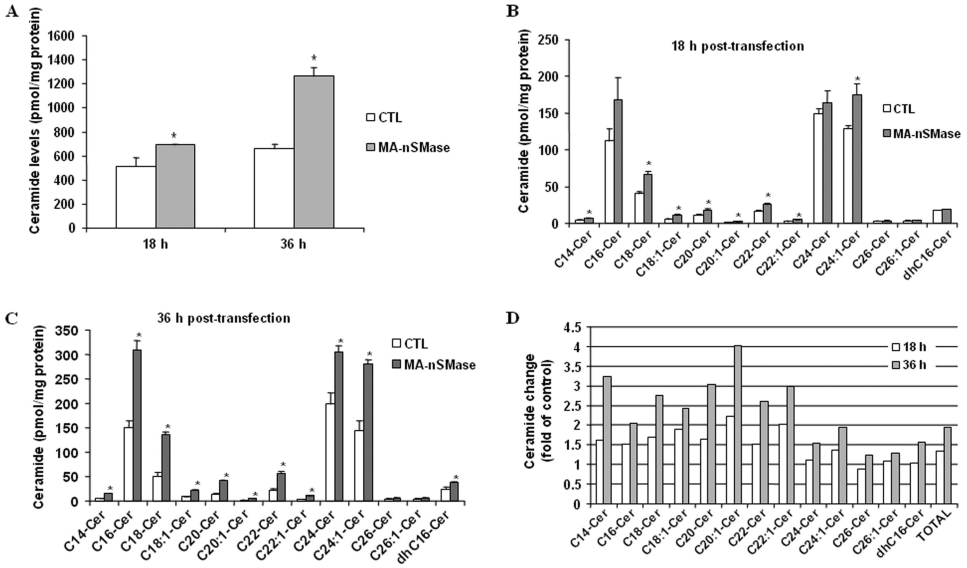

FIGURE 7. **Modulation of ceramide levels by overexpression of MA-nSMase in HEK293 cells.** Changes in ceramide species were analyzed 18 and 36 h after cells were transfected by control (*CTL*) pcDNA3 or MA-nSMase vector. *A*, total ceramide. *B*, ceramide (*Cer*) profiles at 18 h after transfection. *C*, ceramide profiles at 36 h after transfection. *D*, -fold change of ceramide profiles in MA-nSMase-transfected cells compared with control cells. Each sample was normalized to its respective total protein levels. The values are expressed as the mean ± S.D. ($n = 3$). Statistical significance was calculated with respect to control (*, $p < 0.05$). The data are representative of two independent experiments.

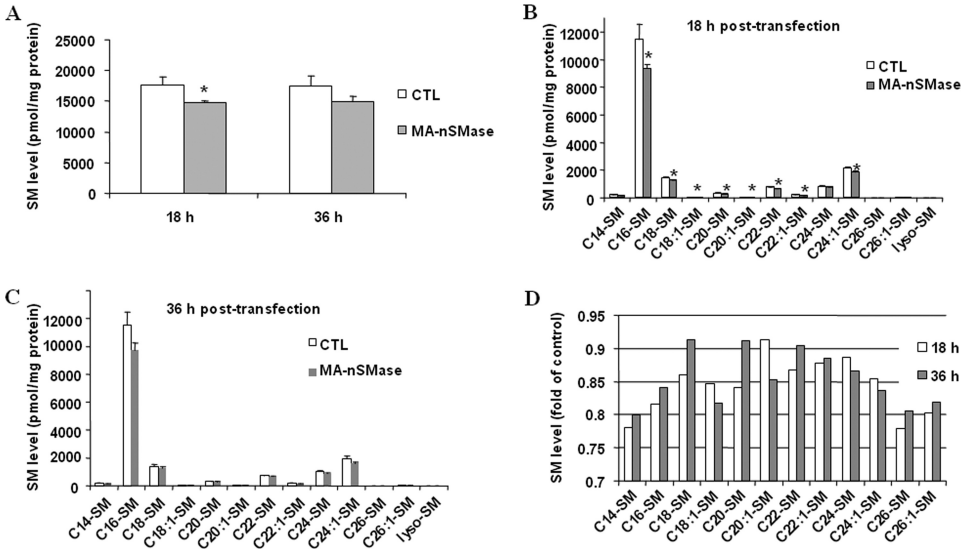

FIGURE 8. **Modulation of SM levels by overexpression of MA-nSMase using HEK293 cells.** Changes in SM species were analyzed 18 and 36 h after cells were transfected with control (*CTL*) pcDNA3 or MA-nSMase vectors. *A*, total SM. *B*, SM profiles at 18 h after transfection. *C*, SM profiles at 36 h after transfection. *D*, -fold change of SM profiles in MA-nSMase-transfected cells of control cells. Each sample was normalized to its respective total protein levels. The values are expressed as the mean ± S.D. ($n = 3$). Statistical significance was calculated with respect to control (*, $p < 0.05$). The data are representative of two independent experiments.

Biochemically, MA-nSMase showed dependence on PS, PG, or CL for *in vitro* activity. CL showed the most effective activation (lowest K_a and highest V_{max}), suggesting that it may be the relevant activator. Notably, CL and PG are both mitochondria-specific phospholipids. Moreover, CL plays important roles in mitochondrial respiration and may be involved in mitochondrial outer membrane permeabilization and release of apoptogenic factors, such as cytochrome *c*, during programmed cell death (33). Thus, the dependence on anionic phospholipids may have implications for the cellular activation of the enzyme. This may also offer some insight into the potential roles of MA-nSMase. However, further studies on MA-nSMase regulation are required before firmer conclusions can be made.

The highest expression of MA-nSMase level was found in testis (Fig. 2), which is distinct from other mammalian nSMases. Interestingly, high N-SMase activity (albeit still lower than that of brain) was observed in testis about 30 years ago (34), but it has remained unclear which nSMase localized in this tissue. Additionally, a manganese-stimulated N-SMase activity was also observed in seminiferous tubules, the specific location of meiosis, suggesting potential roles of nSMase in generation of gametes (35). In that study, the reported SMase activity was optimum at pH 7.4, and it was stimulated by Mn^{2+} more robustly than Mg^{2+}, properties that match those found in this study for MA-nSMase. In rat epididymal spermatozoa, an active divalent cation-dependent SMase activity has also been observed and was implicated in the physiological events preceding fertilization (36). Separate studies have also demonstrated a critical role for SM/ceramide conversion in sperm maturation and function. In the acid SMase knock-out mouse, SM was elevated, and sperm motility was seriously affected, nor did the sperm undergo proper capacitation (37). It is noteworthy that neither ceramide production in the testis nor the ability of the germ cells to undergo apoptosis was affected in the acid SMase KO mouse (38). Thus, the identification of MA-nSMase may provide further insight for sphingolipid metabolism and function in sperm and testis.

Given the significance of the mitochondria in regulation of cell death and the suggested roles of ceramide metabolism in this process, the localization of MA-nSMase raises the possibility that this enzyme functions as a specific regulator of sphingolipid levels in mitochondria and mitochondria-associated membranes. An *in vivo* study demonstrated that ceramide accumulation in mitochondria is required for regulating radiation-induced apoptosis in the germ line of *Caenorhabditis elegans* (25). Previous studies have demonstrated that sphingolipids are important for mitochondrial function. In isolated mitochondria, C_2-ceramide directly inhib-

ited mitochondrial respiratory chain function (39). Moreover, accumulation of endogenous ceramide by targeting bacterial SMase to mitochondria caused Bax translocation to mitochondria, cytochrome *c* release, and cell death (40, 41). More recently, studies have reported that Bax preferentially associates with mitochondrial membrane microenvironments enriched in ceramide (26) and have also indicated that ceramide increases the membrane permeability of isolated mitochondria for cytochrome *c* release (42). Moreover, ceramide can form channels in mitochondrial outer membranes within the concentration range that is present in mitochondria during the induction phase of apoptosis (43), and additional studies showed that both recombinant human Bcl-x(L) and a *C. elegans* Bcl-2 homologue can disassemble ceramide channels in the mitochondrial outer membranes of isolated mitochondria from rat liver and yeast. Taken together, these data suggest that ceramide may be important for releasing proapoptotic proteins from mitochondria during apoptosis (44).

Currently, it remains unclear whether mitochondrial sphingolipids are generated within the organelle itself or whether this occurs in other cellular compartments and is subsequently transported to the mitochondria outer membrane. It is possible that sphingolipids can traffic between mitochondria-associated membranes and mitochondria (45). A study has also suggested that endosomal vesicles trafficking through the cytoskeleton may also play roles in transporting sphingolipids to mitochondria (46). However, the investigation of mitochondrial sphingolipids and their regulation is greatly limited by the lack of knowledge of mitochondrial sphingolipid enzymes, particularly those regulating SM and ceramide metabolism. The identification of MA-nSMase in this study therefore provides an important tool for investigating the regulation of SM and ceramide in mitochondria.

However, it should be noted that the ectopically expressed protein may not completely reflect the roles of the endogenous enzyme. To fully explore the roles of MA-nSMase both in sphingolipid metabolism and physiologically, the generation of MA-nSMase knock-out mice and specific MA-nSMase antibodies will be essential. These tools will also be necessary to determine whether endogenous MA-nSMase is involved in ceramide generation in and around the mitochondria during the induction phase of apoptosis.

In conclusion, this study reports the first isolation of a full-length cDNA encoding a mammalian MA-nSMase. This sheds further light on the compartmentalization of sphingolipid metabolism in mammalian cells. Furthermore, the cDNA sequence of MA-nSMase reported here could allow the generation of MA-nSMase knock-out mice, which would be immensely useful in defining the *in vivo* function of MA-nSMase. Given the crucial role of the mitochondria in the induction of apoptosis, as well as the reported involvement of ceramide in this process, the identification of MA-nSMase may provide a potential "missing" link involved in the regulation of cell death. However, considerable further studies are needed to fully address both the mechanisms of its regulation in response to stimuli as well as the role of this enzyme in stress-induced ceramide generation and subsequent downstream pathways.

Acknowledgments—We thank Drs. Cungui Mao and Ashley Snider for expert advice and assistance. We also thank the Lipidomics Core at the Medical University of South Carolina for mass spectrometry analysis of lipids. The core facility is supported by National Institutes of Health Grants P20 RR0176677 and P01-CA97132.

REFERENCES

1. Hannun, Y. A., and Obeid, L. M. (2008) *Nat. Rev. Mol. Cell Biol.* **9,** 139–150
2. Modrak, D. E., Gold, D. V., and Goldenberg, D. M. (2006) *Mol. Cancer Ther.* **5,** 200–208
3. Chalfant, C. E., and Spiegel, S. (2005) *J. Cell Sci.* **118,** 4605–4612
4. El Alwani, M., Wu, B. X., Obeid, L. M., and Hannun, Y. A. (2006) *Pharmacol. Ther.* **112,** 171–183
5. Nikolova-Karakashian, M., Karakashian, A., and Rutkute, K. (2008) *Subcell. Biochem.* **49,** 469–486
6. Clarke, C. J., Snook, C. F., Tani, M., Matmati, N., Marchesini, N., and Hannun, Y. A. (2006) *Biochemistry* **45,** 11247–11256
7. Clarke, C. J., and Hannun, Y. A. (2006) *Biochim. Biophys. Acta* **1758,** 1893–1901
8. Tomiuk, S., Zumbansen, M., and Stoffel, W. (2000) *J. Biol. Chem.* **275,** 5710–5717
9. Sawai, H., Domae, N., Nagan, N., and Hannun, Y. A. (1999) *J. Biol. Chem.* **274,** 38131–38139
10. Yabu, T., Imamura, S., Yamashita, M., and Okazaki, T. (2008) *J. Biol. Chem.* **283,** 29971–29982
11. Hofmann, K., Tomiuk, S., Wolff, G., and Stoffel, W. (2000) *Proc. Natl. Acad. Sci. U.S.A.* **97,** 5895–5900
12. Marchesini, N., Luberto, C., and Hannun, Y. A. (2003) *J. Biol. Chem.* **278,** 13775–13783
13. Hayashi, Y., Kiyono, T., Fujita, M., and Ishibashi, M. (1997) *J. Biol. Chem.* **272,** 18082–18086
14. Clarke, C. J., Truong, T. G., and Hannun, Y. A. (2007) *J. Biol. Chem.* **282,** 1384–1396
15. Clarke, C. J., Guthrie, J. M., and Hannun, Y. A. (2008) *Mol. Pharmacol.* **74,** 1022–1032
16. Krut, O., Wiegmann, K., Kashkar, H., Yazdanpanah, B., and Krönke, M. (2006) *J. Biol. Chem.* **281,** 13784–13793
17. Stoffel, W., Jenke, B., Blöck, B., Zumbansen, M., and Koebke, J. (2005) *Proc. Natl. Acad. Sci. U.S.A.* **102,** 4554–4559
18. Aubin, I., Adams, C. P., Opsahl, S., Septier, D., Bishop, C. E., Auge, N., Salvayre, R., Negre-Salvayre, A., Goldberg, M., Guénet, J. L., and Poirier, C. (2005) *Nat. Genet.* **37,** 803–805
19. Ardail, D., Popa, I., Alcantara, K., Pons, A., Zanetta, J. P., Louisot, P., Thomas, L., and Portoukalian, J. (2001) *FEBS Lett.* **488,** 160–164
20. Tserng, K. Y., and Griffin, R. (2003) *Anal. Biochem.* **323,** 84–93
21. Yabu, T., Shimuzu, A., and Yamashita, M. (2009) *J. Biol. Chem.* **284,** 20349–20363
22. Novgorodov, S. A., and Gudz, T. I. (2009) *J. Cardiovasc. Pharmacol.* **53,** 198–208
23. Futerman, A. H. (2006) *Biochim. Biophys. Acta* **1758,** 1885–1892
24. Birbes, H., El Bawab, S., Obeid, L. M., and Hannun, Y. A. (2002) *Adv. Enzyme Regul.* **42,** 113–129
25. Deng, X., Yin, X., Allan, R., Lu, D. D., Maurer, C. W., Haimovitz-Friedman, A., Fuks, Z., Shaham, S., and Kolesnick, R. (2008) *Science* **322,** 110–115
26. Martínez-Abundis, E., Correa, F., Pavón, N., and Zazueta, C. (2009) *Febs. J.* **276,** 5579–5588
27. Sawai, H., Okamoto, Y., Luberto, C., Mao, C., Bielawska, A., Domae, N., and Hannun, Y. A. (2000) *J. Biol. Chem.* **275,** 39793–39798
28. Corcoran, C. A., He, Q., Ponnusamy, S., Ogretmen, B., Huang, Y., and Sheikh, M. S. (2008) *Mol. Cancer Res.* **6,** 795–807
29. Muller, P. Y., Janovjak, H., Miserez, A. R., and Dobbie, Z. (2002) *BioTechniques* **32,** 1372–1374, **1376,** 1378–1379
30. Bielawski, J., Szulc, Z. M., Hannun, Y. A., and Bielawska, A. (2006) *Methods* **39,** 82–91

31. Matmati, N., and Hannun, Y. A. (2008) *J. Lipid Res.* **49,** 922–928
32. Kitagaki, H., Cowart, L. A., Matmati, N., Vaena de Avalos, S., Novgorodov, S. A., Zeidan, Y. H., Bielawski, J., Obeid, L. M., and Hannun, Y. A. (2007) *Biochim. Biophys. Acta* **1768,** 2849–2861
33. Gonzalvez, F., and Gottlieb, E. (2007) *Apoptosis* **12,** 877–885
34. Spence, M. W., Burgess, J. K., and Sperker, E. R. (1979) *Brain Res.* **168,** 543–551
35. Raimann, P. E., Custodio de Souza, I. C., Bernard, E. A., and Guma, F. C. (1999) *Mol. Cell. Biochem.* **201,** 125–129
36. Furland, N. E., Oresti, G. M., Antollini, S. S., Venturino, A., Maldonado, E. N., and Aveldaño, M. I. (2007) *J. Biol. Chem.* **282,** 18151–18161
37. Butler, A., He, X., Gordon, R. E., Wu, H. S., Gatt, S., and Schuchman, E. H. (2002) *Am. J. Pathol.* **161,** 1061–1075
38. Otala, M., Pentikäinen, M. O., Matikainen, T., Suomalainen, L., Hakala, J. K., Perez, G. I., Tenhunen, M., Erkkilä, K., Kovanen, P., Parvinen, M., and Dunkel, L. (2005) *Biol. Reprod.* **72,** 86–96
39. Gudz, T. I., Tserng, K. Y., and Hoppel, C. L. (1997) *J. Biol. Chem.* **272,** 24154–24158
40. Birbes, H., El Bawab, S., Hannun, Y. A., and Obeid, L. M. (2001) *FASEB J.* **15,** 2669–2679
41. Birbes, H., Luberto, C., Hsu, Y. T., El Bawab, S., Hannun, Y. A., and Obeid, L. M. (2005) *Biochem. J.* **386,** 445–451
42. Siskind, L. J., Kolesnick, R. N., and Colombini, M. (2002) *J. Biol. Chem.* **277,** 26796–26803
43. Siskind, L. J., Kolesnick, R. N., and Colombini, M. (2006) *Mitochondrion* **6,** 118–125
44. Siskind, L. J., Feinstein, L., Yu, T., Davis, J. S., Jones, D., Choi, J., Zuckerman, J. E., Tan, W., Hill, R. B., Hardwick, J. M., and Colombini, M. (2008) *J. Biol. Chem.* **283,** 6622–6630
45. Voelker, D. R. (2005) *Trends Biochem. Sci.* **30,** 396–404
46. García-Ruiz, C., Colell, A., Morales, A., Calvo, M., Enrich, C., and Fernández-Checa, J. C. (2002) *J. Biol. Chem.* **277,** 36443–36448